Open Journal of Fluid Dynamics, 2026, 16(3), 51-60
https://www.scirp.org/journal/ojfd
ISSN Online: 2165-3860
ISSN Print: 2165-3852

Sounds of Vortex at Low Vortex Mach Numbers

Koichi Takahashi[1,2]

[1]New Industry Creation Hatchery Center, Tohoku University, Sendai, Japan
[2]Research Institute for Data Science, Tohoku Gakuin University, Sendai, Japan
Email: takahashikoichi821@gmail.com

How to cite this paper: Takahashi, K. (2026) Sounds of Vortex at Low Vortex Mach Numbers. *Open Journal of Fluid Dynamics*, **16**, 51-60.
https://doi.org/10.4236/ojfd.2026.163004

Received: June 15, 2026
Accepted: August 15, 2026
Published: August 18, 2026

Copyright © 2026 by author(s) and Scientific Research Publishing Inc.
This work is licensed under the Creative Commons Attribution International License (CC BY 4.0).
http://creativecommons.org/licenses/by/4.0/
Open Access

Abstract

Proper acoustic waves associated with the Rankine vortex of low Mach numbers are studied by solving the compressible Navier-Stokes equations and the continuity equation in cylindrical coordinate system. The vortex Mach number (VMN) is introduced as the ratio of the maximum swirling speed to the sound speed. The density modulation is expressed in terms of the cylindrical functions, which, in contrast to the plane waves, do generally not keep the mass of the fluid invariant. Axisymmetric solutions subjected to mass conservation condition (MCC) are surveyed at low VMN and are shown to exist. The consequence of the MCC is that the wave numbers are complex and discretized in accordance with the distribution of the zeros of the first derivative of the Hankel function. Consequently, the generated sound propagates as a wave packet. The wave length and the width of the wave packet increases and decreases, respectively, with the VMN.

Keywords

Vortex, Sound, Turbulence, Compressible Fluid, Vortex Mach Number, Mass Conservation, Hankel Function

1. Introduction

Vortices are the essential ingredients of turbulence in fluids that we frequently encounter under natural and artificial conditions. In a flow of the Reynolds number Re, turbulence will be observed as random fluctuations of velocity borne by vortices whose sizes may extend over a range of $\mathrm{Re}^{4/3}$ [1]. Impressive phenomena associated with turbulence are the so called "noises" that are not welcome in many occasions of humane lives, and as such, have attracted many researchers' attention in particular in the field of engineering.

Noise of turbulence is an "irregular" sounding due to shear in chaotic flow. The modern theory of sound in turbulence was developed by Lighthill [2] and has been employed and developed by many authors. See, e.g., [3]-[7] and references cited therein. For an informative textbook, see [8] [9].

Lighthill's theory takes account of the irregular turbulent motion of fluid as the source of the density modulation that propagates as sound. The first and the second order velocity fluctuations, which are referred to as the dipole and quadrupole interactions, respectively, constitute the source [2]. The intensity of the sound produced by eddy in such a random way is proportional to the eighth power of the velocity fluctuation and is generally weak.

We may imagine another type of sound whose origin is idiosyncratically tied to a single vortex itself. If a vortex is to generate proper sounds of its own, knowledge on such sounds will help us understand the structures of not only a single vortex but also of turbulence. For such approaches, the perturbative method will be the first step we should take. In meteorology, detecting strong perturbations about steady vortex like typhoon is of a practical theme of research [10] [11]. However, the possibility of small acoustic perturbations propagating from a steady vortex seems not to have been explored systematically.

The purpose of this note is to outline the perturbative approach of sound generation in a vortex with as simple a structure as possible. To this aim, we scrutinize the dynamics of the field fluctuations about the Rankine vortex as the background flow. In the next section, the method of analysis is presented with emphasizing the significance of the requirement that the total mass should be conserved. In Section 3, the result of numerical calculation is presented. Summary and comments are given in the last section.

2. Dynamics of Perturbations around Rankine Vortex

We consider the flow governed by the compressible Navier-Stokes equations

$$\partial_t(\rho\boldsymbol{u})+\partial_i(\rho u_i\boldsymbol{u})=-\nabla p+\eta'\nabla^2\boldsymbol{u}+\left(\zeta+\frac{\eta'}{3}\right)\nabla(\nabla\cdot\boldsymbol{u})+\boldsymbol{f}, \tag{1}$$

and the continuity equation

$$\partial_t\rho+\nabla\cdot(\rho\boldsymbol{u})=0. \tag{2}$$

In (1) and (2), ∂_t and ∂_i denote partial differentiations with respect to the time t and the spatial coordinate component r_i, respectively, ρ the density, $\boldsymbol{u}$ the velocity vector, p the pressure, η' and ζ the viscosity coefficients and $\boldsymbol{f}$ the external force. From (1) and (V2), the density wave equation is derived [2] [8]

$$\partial_t^2\rho-\nabla^2 p=\partial_i\partial_j(\rho u_i u_j)-\eta\nabla^2\nabla\cdot\boldsymbol{u}-\nabla\cdot\boldsymbol{f}, \tag{3}$$

where a new viscosity coefficient has been defined by $\eta\equiv 4\eta'/3+\zeta$. We write the first term on the right-hand side (hereafter, rhs) of (3) as

$$\partial_i\partial_j(\rho u_i u_j)\equiv\mathfrak{D}_{\mathrm{m}}\rho. \tag{4}$$

In cylindrical coordinate system, $\mathfrak{D}_{\mathrm{m}}$ takes the form

$$
\begin{aligned}
\mathfrak{D}_{\mathrm{m}} &= u_r \mathrm{D}\partial_r + \frac{u_\theta^2}{r}\partial_r + u_\theta \mathrm{D}\frac{\partial_\theta}{r} - \frac{u_r u_\theta}{r^2}\partial_\theta + u_z \mathrm{D}\partial_z + 2(\nabla\cdot\boldsymbol{u})\mathrm{D} \\
&+ 2\left((\mathrm{D}u_r)\partial_r + \left(\mathrm{D}\frac{u_\theta}{r}\right)\partial_\theta + (\mathrm{D}u_z)\partial_z\right) + 2(\mathrm{D}\nabla\cdot\boldsymbol{u}) + (\nabla\cdot\boldsymbol{u})^2 \\
&+ (\partial_r u_r)^2 + \left(\frac{\partial_\theta u_\theta}{r}\right)^2 + \left(\frac{u_r}{r}\right)^2 + \frac{2}{r}\partial_r u_\theta \partial_\theta u_r + 2\partial_r u_z \partial_z u_r \\
&+ \frac{2}{r}\partial_\theta u_z \partial_z u_\theta - \frac{2}{r} u_\theta \partial_r u_\theta + \frac{2}{r^2} u_r \partial_\theta u_\theta,
\end{aligned}
\tag{5}
$$

where

$$
\mathrm{D} \equiv \boldsymbol{u}\cdot\nabla = u_r\partial_r + \frac{u_\theta}{r}\partial_\theta + u_z\partial_z .
$$

To simplify the problem, we analyze the system (3) - (5) with no external force for the steady and circular Rankine vortex $\boldsymbol{u} = (0, u_\theta(r), 0)$ as the background flow where

$$
u_\theta(r) = \begin{cases} \Omega r, & r \le R, \\ \Gamma/2\pi r, & r \ge R, \end{cases} \tag{6}
$$

with the relation $\Gamma = 2\pi\Omega R^2$. The maximum flow speed is given by $u_\theta^{\max} = \Omega R$. The vortex undergoes a rigid body rotation in the inner or core region and a motion with a constant circulation in the outer region. The vorticity is distributed in the core region. The Navier-Stokes equations tell us that the pressures at $r = 0$ and $r = \infty$ are related as

$$
p_0(\infty) - p_0(0) = \rho_0 \left(u_\theta^{\max}\right)^2 . \tag{7}
$$

Consider small adiabatic changes (*i.e.*, entropy is conserved):

$$
\rho_0 \to \rho_0 + \rho_1, \quad p_0 \to p_0 + p_1, \quad \boldsymbol{u} \to \boldsymbol{u} + \delta\boldsymbol{u}, \tag{8}
$$

$$
\frac{p_1}{p_0} = \gamma \frac{\rho_1}{\rho_0}, \tag{9}
$$

where γ is the adiabatic index. The sound speed $c(r)$ is given by

$$
c(r)^2 = \gamma \frac{p_0(r)^2}{\rho_0^2} \tag{10}
$$

In (3), assuming the form

$$
\rho_1(\boldsymbol{r}, t) = \mathrm{e}^{\mathrm{i}(-\omega t + m\theta + k_z z)} \tilde{\rho}_1(r), \tag{11}
$$

the equation for $\tilde{\rho}_1(r)$ is obtained. When sound speed is far greater than the flow speed and viscosity is ignored, the equation takes the form of the Bessel type near the origin and far away from the origin but with different parameters in the both regions. Indeed, substituting (6) and (11) to (5) with reference to (10), the Equation (3) and their solutions in the above approximations are given by

$$
\tilde{\rho}_1'' + \frac{1}{r}\tilde{\rho}_1' + \left(\beta^2 - \frac{\mu^2}{r^2}\right)\tilde{\rho}_1 = 0, \tag{12}
$$

$$
\tilde{\rho}_1(r) = Z_\mu(\beta r), \tag{13}
$$

where $Z_\mu(\beta r)$ stands for cylindrical function and

$$\left(\beta^2,\mu^2\right)=\begin{cases}\left(\dfrac{\omega^2}{c_0(\infty)^2}-k_z^2,\ m^2-\dfrac{\gamma\Omega^2R^4\omega^2}{c_0(\infty)^4}\right), & \text{outer region,}\\[2ex] \left(\dfrac{\omega^2}{c_0(0)^2}-\dfrac{\Omega^2}{c_0(0)^2}\left(m^2+2\right)-k_z^2,\ m^2\right), & \text{inner region,}\end{cases} \tag{14}$$

where $c_0(0)$ and $c_0(\infty)$ are the unperturbed sound speed at $r=0$ and ∞, respectively. On the rhs of (14), the upper (lower) columns are for the outer (inner) region.

We write the radial wave number in the outer region as $k_>$. From (14), the wave solutions propagating outward exist when the frequency obeys the dispersion relation

$$\omega(K_>)=\pm c_\infty K_>. \tag{15}$$

where $K_>\equiv\left(k_>^2+k_z^2\right)^{1/2}$, $c_\infty\equiv c_0(\infty)$. When $k_z=0$, writing as $K_>=k_>$, the double signs in (15) can be removed by allowing $k_>$ to take unrestricted complex values. The correction to (15) due to viscosity is the order of $\nu K_>^2$, which is negligible. $\nu\equiv\eta/\rho_0$ is the kinematic viscosity.

Ignoring the viscosity, the solutions in the outer region are well approximated by the Hankel function $H_\mu^{(1)}(k_>r)$ with

$$\mu=\pm\sqrt{m^2-\gamma\left(MRK_>\right)^2},\quad m\ge 0. \tag{16}$$

In the inner region, the solution is given by the Bessel function $J_m(k_<r)$ (and the Neumann function $Y_0(k_<r)$ when $m=0$). In (16), we defined the vortex Mach number (VMN) by $M=u_\theta^{\max}/c_\infty$. The μ is generally complex due to the VMN term in (16). Its origin is traced back to the shear of the kinetic energy $\sim\left(u_\theta^2/2\right)'$ in (5). The double signs in (16) are independent of those in (15) and are reserved in (16). The relation (14) for the inner region also gives the dispersion relation

$$k_<^2=\frac{\omega^2}{c_0(0)^2}-\frac{\Omega^2}{c_0(0)^2}\left(m^2+2\right)-k_z^2. \tag{17}$$

In summary at this stage of the arguments, the outer solution $\tilde{\rho}_>$ and the inner solution $\tilde{\rho}_<$ for $m=0$ are given by

$$\tilde{\rho}_>=CH_\mu^{(1)}(k_>r), \tag{18}$$

$$\tilde{\rho}_<=AJ_0(k_<r)+BY_0(k_<r). \tag{19}$$

These solutions are to be smoothly connected together at $r=R$ (connection condition, CC):

$$AJ_0(k_<R)+BY_0(k_<R)=CH_\mu^{(1)}(k_>R), \tag{20}$$

$$Ak_<J_0'(k_<R)+Bk_<Y_0'(k_<R)=Ck_>H_\mu^{(1)\prime}(k_>R). \tag{21}$$

The CC must be time independent, so that the ω in (17) must coincide with the one given by (15). Hereafter, we restrict ourselves to the case $k_z = 0$ so that $K_> = k_>$.

The asymptotic form of the outer solution is given with a normalization constant C by

$$\begin{aligned}\rho_1(\boldsymbol{r},t) &= C\mathrm{e}^{-\mathrm{i}\omega t+\mathrm{i}m\theta}H_\mu^{(1)}(k_> r)\\ &\to C\sqrt{\frac{2}{\pi k_> r}}\left(1+\mathrm{i}\frac{4\mu^2-1}{8k_> r}+\cdots\right)\exp\left[-\mathrm{i}k_>(c_\infty t - r)+\mathrm{i}\left(m\theta-\frac{2\mu+1}{4}\pi\right)\right].\end{aligned} \tag{22}$$

The wave front is supposed to be at $r = c_\infty t$. Without energy supply, the wave at a fixed r should not intensify. This is possible when $\mathrm{Im}\,k_> \le 0$. In this case, (22) represents a wave packet having the radial width $1/|\mathrm{Im}\,k_>|$.

We further impose a condition that the density modulation has to keep the total mass invariant (mass conservation condition, MCC):

$$I \equiv \int \rho_1(\boldsymbol{r},t)\mathrm{d}\boldsymbol{r} = 0. \tag{23}$$

Note that (23) is fulfilled mathematically for $m \ge 1$ or $k_z \ne 0$. The upper bound of the r-integration in (23) is the position of the wave front. Even under this restriction, the above integration yields a term divergent in t because of the asymptotic form (22). However, the phase of the divergent part can be arbitrarily chosen. This means that the integration (23) is regularized by appropriately choosing the phase of C and taking, e.g., the real part of ρ_1 as the physical solution. Consequently, the physically allowed $k_>$ are given by the zeros of the first derivative of $H_\mu^{(1)}(z)$. See **Appendix**. Then, given a vortex specified by R and M, we have six Equations (20), (21), (23), (16) (15) and (17) that will be solved for six unknowns A/C, B/C, ω, $k_>$, $k_<$ and μ.

3. Result of Numerical Calculation

In this section, for simplicity, we are interested in the modes $m = 0 = k_z$, whose intensities are the lowest for a given $k_>$. We set $R = 1$ in numerical calculations. The result is presented in Figure 1 for axially symmetric mode (*i.e.*, $m = 0$) and small VMNs $0 < M \le 0.17$. ($M = 0.17$ amounts to the wind speed of about 58 m·s^{-1} in the normal atmospheric condition on the earth.) There, five sequences of $k_>$ for the physical solutions, *i.e.*, $\mathrm{Im}\,k_> < 0$, are depicted as functions of M. The solutions for $k_>$ form distinctive sequences. Since the wave number uniquely determines the frequency ω, the figure shows that the VMN determines the tones which form sequences as the VMN varies. Each sequence is labeled by a set of a capital and a corresponding small letter. A capital letter is employed for $\mathrm{Re}\,k_>$ and a small letter for $\mathrm{Im}\,k_>$. The sequence (A, a) is of the fundamental tones and the other sequences are of the overtones. All of $\mathrm{Re}\,k_>$ and $\mathrm{Im}\,k_>$ are negative. The other characteristics of the solutions are summarized below.

(A, a): $\mathrm{Re}\,k_> \approx -0.4$ and $\mathrm{Im}\,k_> \approx -0.6$ are dependent on M very weakly.

(B, b): $\mathrm{Re}\,k_> \approx -4$, $-1.1 < \mathrm{Im}\,k_> < -0.4$. Sound propagates as a wave packet with the wavelength $\lambda \approx \pi/2$ and the spatial width $w \approx 1 \sim 2$. For $w \approx \lambda$, the wave packet will look virtually like a moving lump of pressure deviations.

(C, c), (D, d): $|\mathrm{Re}\,k_>|$ and $|\mathrm{Im}\,k_>|$ are appreciably decreasing and increasing functions of M, respectively. At $M \approx 0$, the spacing of neighboring $\mathrm{Re}\,k_>$ is about π and λ is shorter than 1. On the other hand, since $|\mathrm{Im}\,k_>| \approx 0.35$, w is about 3. For $w/\lambda > 1$, the oscillation of the waves will be observable.

The above feature of (B, b), (C, c) and (D, d) are analogous to the vibration of a medium confined in a box.

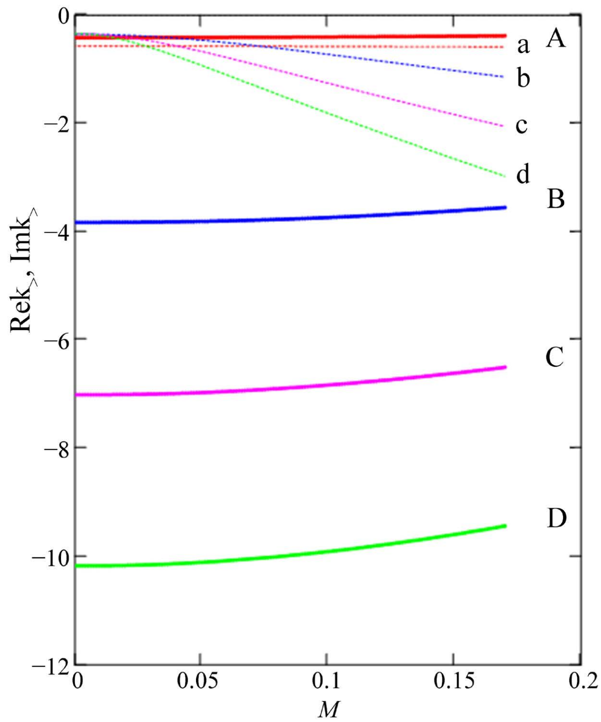

Figure 1. $\mathrm{Re}\,k_>$ and $\mathrm{Im}\,k_>$ vs. M for five sequences of tones. Bold curves are of $\mathrm{Re}\,k_>$ and are labeled by capital roman letters A - E. Thin curves are of $\mathrm{Im}\,k_>$ and are labeled by the corresponding small roman letters a - e. Same color is used for $\mathrm{Re}\,k_>$ and $\mathrm{Im}\,k_>$ of the same solution. Inset: Enlarged drawings for $\mathrm{Re}\,k_>$ (A) and $\mathrm{Im}\,k_>$ (a).

$|\mathrm{Re}\,k_>|$ of all solutions tends to decrease with M. Therefore, the "density of states", *i.e.*, the number of solutions per unit frequency, increases with M. At the same time, $|\mathrm{Im}\,k_>|$ also tends to increase. Consequently, the Rankine vortex with larger Mach number will be able to generate more compact wave packets.

4. Summary and Comments

We examined within the compressible Navier-Stokes equations in cylindrical coordinate system whether proper radially traveling acoustic waves are supported by the steady Rankine vortex. With some presumably pertinent approximations, we found for the axially symmetric mode that

1) The radially traveling sounds proper to the Rankine vortex exist, each of

which is characterized by a radial wave number.

2) The radial wave number depends on the VMN.

3) The radial wave number is complex owing to the MCC. The complex μ also plays a part in developing the imaginary part of the wave number.

4) Imaginary part of the radial wave number originates from the complex zeros of the Hankel function together with the shear in the kinetic energy of the background vortex flow and remains finite in inviscid limit.

5) Physical wave packets form and travel to the radial direction when the imaginary part of the wave number is negative.

Proper sounds are characterized by the discrete complex wave numbers and frequencies. Subtle adjustment of the positions of the nodes and the amplitude of the wave is needed to fulfill the MCC. The MCC comes to time-independent fulfillment by the propagation of sound in the form of wave packet whose form is essentially not altered during the propagation. Owing to the proper sounds, resonance will take place when the vortex is subjected to external acoustic stimulations with corresponding frequencies.

In view of practical applications, one may ask what if the azimuthal velocity component u_θ is a smooth function. This is not an easy problem. Besides heavy numerical calculations, one possibility may be as follows. Suppose that we could somehow find a Rankine vortex function $u_\theta^{(0)}$ such that the difference $\delta u_\theta = u_\theta - u_\theta^{(0)}$ is minimized in a certain sense. If we could solve the wave equation perturbatively in δu_θ, we would in principle have the perturbative corrections to the wave numbers that had been found as the zeros of the first derivative of the Hankel function as is the case with the present study.

Compression and extension of the flow are not involved in the Rankine vortex but also contribute to the kinetic energy. A question to be addressed is therefore: what happens in other vortices like Burgers' [12]? An interesting possibility will also arise that the proper sounds from turbulence may convey nontrivial information on the distribution of vortices. These are left for future study.

Conflicts of Interest

The author declares no conflicts of interest regarding the publication of this paper.

References

[1] Davidson, P.A. (2015) Turbulence. Oxford University Press. https://global.oup.com/academic/product/turbulence-9780198722595?cc=jp&lang=en&

[2] Lighthill, M.J. (1952) On Sound Generated Aerodynamically I. General Theory. *Proceedings of the Royal Society of London. Series A. Mathematical and Physical Sciences*, **211**, 564-587. https://doi.org/10.1098/rspa.1952.0060

[3] Proudman, I. (1954) The Generation of Noise by Isotropic Turbulence. *Proceeding of the Royal Society of London*, **214**, 119-132. https://www.semanticscholar.org/paper/The-generation-of-noise-by-isotropic-turbulence-Taylor/618ab5dbb157cd85ae7862f1d019cfad174b6de5

[4] Lilley, G.M. (1994) The Radiated Noise from Isotropic Turbulence. *Theoretical and Computational Fluid Dynamics*, **6**, 281-301. https://doi.org/10.1007/bf00311842

[5] Dowling, A.P. and Hynes, T.P. (2004) Sound Generation by Turbulence. *European Journal of Mechanics—B/Fluids*, **23**, 491-500. https://doi.org/10.1016/j.euromechflu.2003.10.014

[6] Terakado, D., Nonomura, T., Kawai, S., Aono, H., Sato, M., Oyama, A., *et al*. (2022) Sound Source Characteristics Generated by Shocklets in Isotropic Compressible Turbulence. *Physical Review Fluids*, **7**, Article ID: 084605. https://doi.org/10.1103/physrevfluids.7.084605

[7] Routh, S. and Musielak, Z.E. (2025) Lighthill's Theory of Sound Generation in Non-Isothermal and Turbulent Fluids. *Fluids*, **10**, Article 156. https://doi.org/10.3390/fluids10060156

[8] Howe, M.S. (2002) Theory of Vortex Sound. Cambridge University Press. https://doi.org/10.1017/cbo9780511755491

[9] Raichel, D.R. (2006) The Science and Applications of Acoustics. Springer.

[10] Mashiko, W. and Shimada, U. (2021) Observed Near-Surface Wind Structure in the Inner Core of Typhoon Goni (2015). *Monthly Weather Review*, **149**, 1785-1800. https://doi.org/10.1175/mwr-d-20-0294.1

[11] Feng, Y., Wu, L., Liu, Q. and Zhou, W. (2021) Negative Pressure Perturbations Associated with Tornado-Scale Vortices in the Tropical Cyclone Boundary Layer. *Geophysical Research Letters*, **48**, e2020GL091339. https://doi.org/10.1029/2020gl091339

[12] Burgers, J.M. (1948) A Mathematical Model Illustrating the Theory of Turbulence. *Advances in Applied Mechanics*, **1**, 171-199. https://doi.org/10.1016/s0065-2156(08)70100-5

[13] Döring, B. (1966) Complex Zeros of Cylinder Functions. *Mathematics of Computation*, **20**, 215-222. https://www.semanticscholar.org/paper/Complex-zeros-of-cylinder-functions-D%C3%B6ring/38402dc30b2c45c943a1d7a0aeb9eda5809361a3

[14] Cruz, A. and Sesma, J. (1982) Zeros of the Hankel Function of Real Order and of Its Derivative. *Mathematics of Computation*, **39**, 639-645. https://doi.org/10.1090/s0025-5718-1982-0669655-8

Appendix

The MCC (23) is divided into two parts:

$$I = I_{\text{in}} + I_{\text{out}} = 0, \tag{A1}$$

where

$$\begin{aligned} I_{\text{in}} &= \int_0^R \mathrm{e}^{-\mathrm{i}\omega t} \tilde{\rho}_< r\mathrm{d}r, \\ I_{\text{out}} &= \int_R^{c_\infty t} \mathrm{e}^{-\mathrm{i}\omega t} \tilde{\rho}_> r\mathrm{d}r, \end{aligned} \tag{A2}$$

where $\tilde{\rho}_<$ and $\tilde{\rho}_>$ are the functions of r only. (Strictly speaking, the deviation of $\rho_1(\mathbf{r},t)$ from the asymptotic from (22) will occur near the wave front and also contributes to I. We assume that this contribution is negligible.)

The inner part I_{in} is given by an integration of the Bessel function and the Neumann function, while I_{out} is given by an integration of the Hankel function as are seen from (19) and (18). I_{in} is finite and is given by

$$I_{\text{in}} = \mathrm{e}^{-\mathrm{i}\omega t} \int_0^R \left(\frac{A}{C} J_0(k_< r) + \frac{B}{C} Y_0(k_< r) \right) r\mathrm{d}r = -\mathrm{e}^{-\mathrm{i}\omega t} \frac{k_> R}{k_<^{\,2}} \frac{\mathrm{d}H_\mu^{(1)}(z)}{\mathrm{d}z} \bigg|_{z=k_> R}. \tag{A3}$$

In deriving (A3), uses have been made of the relations readily obtained from (20) and (21):

$$\frac{A}{C} = \frac{1}{D} \begin{vmatrix} H_\mu^{(1)}(k_> R) & Y_0(k_< R) \\ (k_>/k_<) H_\mu^{(1)\prime}(k_> R) & Y_0'(k_< R) \end{vmatrix}, \tag{A4}$$

$$\frac{B}{C} = \frac{1}{D} \begin{vmatrix} J_0(k_< R) & H_\mu^{(1)}(k_> R) \\ J_0'(k_< R) & (k_>/k_<) H_\mu^{(1)\prime}(k_> R) \end{vmatrix}, \tag{A5}$$

where, by virtue of Lommel's formula,

$$D \equiv \begin{vmatrix} J_0(k_< R) & Y_0(k_< R) \\ J_0'(k_< R) & Y_0'(k_< R) \end{vmatrix} = \frac{2}{\pi k_< R}. \tag{A6}$$

From the asymptotic form (22) of the Hankel function, we can estimate the time dependence of I_{out} as

$$I_{\text{out}}(t) \sim C\sqrt{\frac{2}{\pi k_>^3}} \mathrm{e}^{-\mathrm{i}(2\mu+1)\pi/4} \left[-\mathrm{i}(c_\infty t)^{1/2} + \frac{4\mu^2+3}{8k_>(c_\infty t)^{1/2}} + O\left((c_\infty t)^{-3/2}\right) \right]. \tag{A7}$$

The term divergent for $t \to \infty$ in the brackets is pure imaginary and the non-divergent term is complex. Suppose that β^2 and μ^2 are dominantly real (this is true for the most of the solutions as is shown in Section 3.) and remember that the real or the imaginary part of $\rho_1(\boldsymbol{r},t)$ (or their linear combination without spatio-temporal dependence) can be the solution. Then, by appropriately choosing the phase of the constant C so as to cancel the phase factor in $k_>^{-3/2}\mathrm{e}^{-\mathrm{i}(2\mu+1)\pi/4}$ and by choosing the real part of $\rho_1(\boldsymbol{r},t)$, the divergence due to $(c_\infty t)^{1/2}$ in I_{out} is removed. The remaining terms converge to zero. Together with (A1) and (A3), it turns out what we need is to solve the condition

$$\left.\frac{\mathrm{d}H_{\mu}^{(1)}(z)}{\mathrm{d}z}\right|_{z=k_{>}R} = 0, \tag{A8}$$

i.e., the zeros of the first derivative of $H_{\mu}^{(1)}(z)$. They are generally complex [13] [14]. For numerical calculations involving the cylindrical functions with complex order, their integral representations were used.